Two good metals make a semiconductor: A potassium-nickel compound under pressure

Adebayo A. Adeleke,[1] Elissaios Stavrou,[2] Adebayo O. Adeniyi,[1] Biao Wan,[3,4] Huiyang Gou,[3] and Yansun Yao[1,*]

[1]*Department of Physics and Engineering Physics, University of Saskatchewan, Saskatoon, Saskatchewan, Canada S7N 5E2*
[2]*Lawrence Livermore National Laboratory, Physical and Life Sciences Directorate, Livermore, California 94550, USA*
[3]*Center for High Pressure Science and Technology Advanced Research, Beijing 100094, China*
[4]*State Key Laboratory of Metastable Materials Science and Technology, Yanshan University, Qinhuangdao 066004, China*

(Received 28 February 2020; revised 10 October 2020; accepted 13 October 2020; published 29 October 2020)

We predict a potassium-nickel intermetallic compound K_2Ni at high pressure and identify it as the long-sought structure of the only known K-Ni compound to date [Parker *et al.*, Science **273**, 95 (1996)]. Although both constituent elements are metallic, K_2Ni exhibits a semiconducting ground state with an indirect band gap of 0.65 eV. Electron instability due to the degeneracy at the Fermi level arises from the particular motif of the structure, which in turn induces symmetry-breaking Peierls distortion and a nonmetallic ground state. The results indicate that the chemical properties of elements can change dramatically under extreme conditions and have significant implications for the postulation that potassium is incorporated in Earth's core.

DOI: 10.1103/PhysRevB.102.134120

I. INTRODUCTION

The alkali metals have long been considered as simple metals. In their pioneering work [1], Wigner and Seitz introduced a description of nearly free electron (NFE) metal, in which the valence electrons are only weakly perturbed by a periodic positive background. This behavior of valence electrons was soon recognized in many metals, especially in group-I elements classified as simple metals. Indeed, all group-I elements from Li to Cs adopt body-centered-cubic (bcc) structure, a prototypical structure for NFE metals. Solid hydrogen is the only exception; its protons would pair to H_2 molecules and form an insulating ground state. But it is anticipated that under extreme pressure hydrogen will adopt nonmolecular structures and become metallic, just like other alkali metals [2,3]. Compressing hydrogen until it becomes metallic is a holy grail of physics, and there are strong evidences supporting the finding of metallic hydrogen in the laboratory [4–6]. Amazingly, under high pressure alkali metals can also depart from NFE behavior and reach a nonmetallic state by the increasing effects of Pauli exclusion and orthogonality with rising electron density [7–9], which is against the intuitive expectations of quantum mechanics that the NFE metals should become even more free-electron-like at higher densities. Lithium, especially, can act a bit like hydrogen and form diatomic-molecule-like structures under high pressure [7,10]. The similarity of dense alkali metals to solid hydrogen is compelling, which suggests the distinct possibility of a nonmetallic state in the alloys of the former. As we will show in this paper, a semiconducting ground state can be obtained in alloys of alkali metals, exemplified here by a potassium-nickel compound, K_2Ni. The idea of combining two good metals to form a semiconductor is interesting, which is achieved at high pressure where K and Ni atoms are modulated into Peierls states similar to pure hydrogen.

Potassium-nickel compounds have merits in science from a fundamental point of view. K and Ni do not form compounds at ordinary conditions due to the large difference in their charge densities (Miedema's rule [11]). Although K and Ni are abundant in Earth's crust, the chemistry of elements at ambient pressure is not applicable to the pressure beyond moderate depths. Pressure can alter the properties of elements and lead to the formation of new compounds [12]. At high pressures, K departs significantly from a NFE metal through an *s*-to-*d* transition [13], that is, valence electrons initially in the 4*s* orbital start to populate 3*d* orbitals due to the change of orbital energies in reduced space. Theoretical calculation suggests that K can attain an *s*-band ferromagnetic ground state in open structures under high pressure [14]. As such, K becomes a transition-metal-like element and is able to form compounds with another transition metal, e.g., Ag and In [15,16]. Geophysicists have long postulated that K may also react with Fe and Ni, the major components of the Earth's core, at the physical conditions of the Earth's core [17]. This theory is to explain the discrepant values of K/U ratios estimated for the Earth and that measured in chondrites and terrestrial rocks, which suggests that the "missing" K has sequestered into the accreting core [18]. Some twenty years ago, Parker *et al.* synthesized a crystalline phase of K-Ni above 30 GPa, but could not determine its crystal structure [19]. Also, a possible chemical reaction between K and Fe has been modelled theoretically in a solid solution at 35 GPa [20,21]. These studies could shine light on the partitioning of trace elements between the Earth's core and the mantle, a key problem in the evolution of Earth, but a lack of the knowledge of the crystal structures limits our understanding. In this study, we systematically investigate the potential-energy landscape of the K-Ni system using global structure search methods and found several stable K_xNi_y stoichiometries at high

*yansun.yao@usask.ca

pressure. We predict a stable polymorph of K_2Ni whose structure sufficiently explains the observation of the K-Ni compound synthesized by Parker *et al.*, by fitting the diffraction lines. The predicted K_2Ni compound has a semiconducting ground state. We further establish that an interplay between electron instability and structural distortion stabilizes this compound and eventually opens an energy band gap, giving it a nonmetallic property.

II. METHODS

A search for stable structures was carried out using two global search methods: genetic algorithm (GA) [22] and particle swarm-intelligence optimization (PSO) [23,24]. The search was done at 0 and 37 GPa (i.e., synthesis pressure for K-Ni compound [19]) with simulation cells containing up to four K_xNi_y formula units. Geometrical optimization, total-energy calculation, and molecular dynamics (MD) simulation were performed using the Vienna *ab initio* simulation package (VASP) [25] and projector-augmented wave (PAW) potentials [26] with the Perdew-Burke-Ernzerhof (PBE) functional [27]. The K and Ni potentials were employed with valence states of $3s^23p^64s^1$ and $3s^23p^63d^84s^2$, respectively, and an energy cutoff of 450 eV. A k spacing of $2\pi \times 0.02\,\text{Å}^{-1}$ was used for Brillouin zone (BZ) sampling. The energy difference between different magnetic states for the energy minimum structure is expected to be small, therefore, structure search, phonon, and MD calculations were done without spin polarization. Phonons were calculated using the density functional perturbation theory as implemented in the VASP code and the calculated force constants were postprocessed using the PHONOPY code [28]. *Ab initio* molecular dynamics (AIMD) simulations were performed employing an isothermal-isobaric (*NPT*) ensemble in a 3×3×3 supercell with 162 atoms. MD trajectories were obtained from 10-ps-long simulations sampled with a 2-fs time step. The system temperature was controlled using the Langevin thermostat. The finite temperature vibrational density of states (vDOS) was obtained from the velocity autocorrelation function (VACF) of the MD trajectories [29]. Thermodynamic stability of predicted K_xNi_y structures were examined using their enthalpies of formation (ΔH_f) with respect to the solid mixture of K and Ni at the same pressure, i.e., $\Delta H_f(K_xNi_y) = [H(K_xNi_y) - xH(K) - yH(Ni)]/(x+y)$. A global stability tie line (convex hull) in stoichiometry space is constructed using ΔH_f of the most stable structures for all compositions.

Since hybrid functionals predict an energy-band gap more accurately than semilocal density functionals such as PBE, electronic band structure and electron localization function (ELF) calculations were done using the Heyd-Scuseria-Ernzerhof (HSE) hybrid functional [30] with a mixing parameter of 0.25 as implemented in the VASP code. ELF calculation was performed using a 120×120×120 mesh. The crystal-orbital Hamilton-population (COHP) and integrated COHP (ICOHP) analysis was performed with an HSE functional based electronic structure calculation using the LOBSTER code [31]. Magnetic (spin-polarized quantum) calculations were performed on a model built from a 2×2×2 supercell comprising of 48 atoms. The ferromagnetic, ferrimagnetic, antiferromagnetic, and paramagnetic configurations were constructed and their ground-state energies calculated within GGA + U approximation using the PBE functional. The correlation effect on $3d$ electrons was treated within the GGA + U using the Dudarev approach [32] with an on-site Coulomb interaction U_{eff} ($U_{\text{eff}} = U - J$) of 5.0 eV, which is according to the U_{eff} value proposed for Ni [33] where linear-response theory was used. Structures are visualized using the VESTA code [34].

III. RESULTS AND DISCUSSION

The convex hull calculated at 37 GPa [Fig. 1(a)] suggests that several K_xNi_y stoichiometries become thermodynamically stable with respect to elemental K and Ni. This list includes K_4Ni, K_2Ni, K_3Ni_2, K_3Ni_4, and KNi_4, all unknown before but accessible through synthesis according to this calculation. The convex hull calculated at 0 GPa (see the Supplemental Material [35]) reveals no thermodynamically stable K-Ni compounds. K-Ni compounds are therefore strictly high-pressure phases. The predicted stoichiometries/structures at 37 GPa are screened by comparing their x-ray-diffraction patterns to the experimental pattern of the K-Ni compound reported by Parker *et al.* [19]. One monoclinic structure of K_2Ni, with the $P2_1/m$ space group, turns out to be a very good match [Fig. 1(b)]. The evolution of ΔH_f under pressure for K_2Ni predicts a formation pressure of ~17 GPa [35]. This structure is similar to the $EuSb_2$, with the same space group. In this interpretation, the experimental XRD pattern should have contributions from $P2_1/m$-K_2Ni, and some unreacted starting material (elemental K and Ni). All of the signature peaks of the K-Ni compound can be indexed to $P2_1/m$-K_2Ni. In addition, the peak at $2\theta = 24.8^\circ$ can be uniquely indexed to fcc-Ni, while the peak at $2\theta = 21.4^\circ$ appears to be an overlap of a stronger peak from fcc-Ni and a minor peak from the $P2_1/m$-K_2Ni. The two peaks at $2\theta = 20.2^\circ$ and $2\theta = 20.5^\circ$ belong to the K-III structure. Since K-III is an incommensurate structure, we cannot simulate its XRD pattern, but nonetheless there are no peaks from $P2_1/m$-K_2Ni or fcc-Ni occupying these two spots. Essentially, most of the 2θ positions and relative intensities of the Bragg peaks in the experimental XRD can be matched to the theoretical structures. The small deviation in the intensities could be due to the uncertainties in both experiment and theory.

Experimentally, the K-Ni compound has been synthesized from K and Ni powder mixed in a molar ratio of 2:1 at the same pressure [19]. Thus, the identification of a K_2Ni stoichiometry should not be a coincidence. Also noted is that the $P2_1/m$ structure is slightly above the global stability tie line [red dot, Fig. 1(a)], suggesting that this structure is a metastable one. The thermodynamic ground state of K_2Ni is predicted to be an orthorhombic structure with the *Cmcm* space group [black dot, Fig. 1(a)], which has an enthalpy of 0.02 eV/atom lower than the $P2_1/m$ structure with zero-point energy (ZPE) included. Since the experimental synthesis has been carried out at high temperature (2000– ~ 2500 K) by laser heating, the product should be a compound that is stabilized at high temperatures. To account for temperature effects, the free energies of the structures were calculated within the

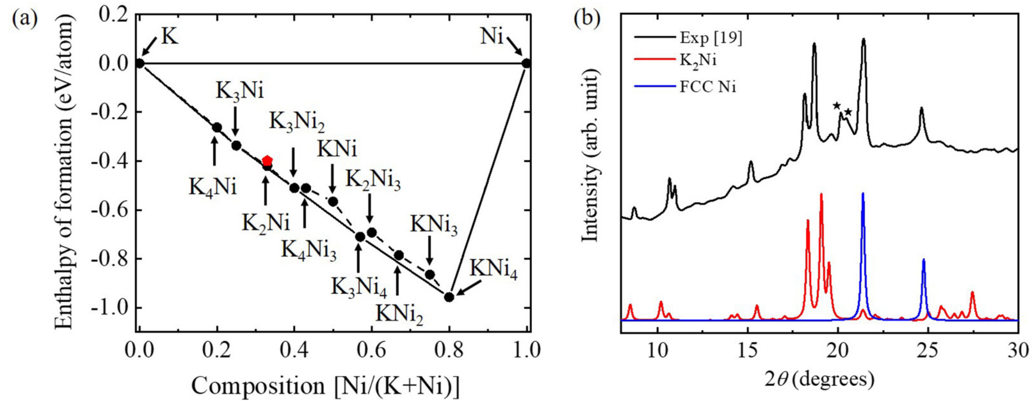

FIG. 1. (a) Enthalpy of formation of various K-Ni compounds with respect to constituent elemental decomposition at 37 GPa. (b) Calculated XRD patterns for the $P2_1/m$-K_2Ni and the fcc-Ni at 37 GPa, compared with the previous reported experimental XRD pattern [19] at the same pressure. The x-ray wavelength used is $\lambda = 0.72$ Å. Asterisks indicate the positions of K-III peaks at 30 GPa (slightly shifted downward due to volume difference).

hamonic approximation [39],

$$F(T) = E_0 + k_B T \int_0^\infty g(\omega) \ln \left[2 \sinh \left(\frac{\hbar\omega}{2k_B T} \right) \right] d\omega, \quad (1)$$

where E_0 is the static crystal energy and the second term is the vibrational free energy F_{vib}; ω is the phonon frequency and $g(\omega)$ is the phonon density of states (DOS), calculated using the fixed volume obtained at 0 K. The calculated free energies reveal that the *Cmcm*-K_2Ni is only preferred at low temperatures up to ∼750 K while $P2_1/m$-K_2Ni becomes more stable at temperatures above ∼1000 K [35]. In the intermediate region, the energy difference between these two structures is not distinguishable. This finding establishes the $P2_1/m$-K_2Ni phase as one that is more accessible at high temperatures, which is consistent with the synthesis conditions.

The crystal structure of $P2_1/m$-K_2Ni is shown in Fig. 2(a). The optimized structural parameters at 37 GPa are $a = 5.21$ Å, $b = 4.25$ Å, $c = 4.35$ Å, and $\beta = 111.37^\circ$ with K atoms located at 2*e*: 0.669, 0.75, 0.087; 2*e*: 0.015, 0.75, 0.764; and Ni atoms at 2*e*: 0.622, 0.25, 0.573. The alloying between K and Ni is achieved by the changes in chemical and electronic structures at high densities. Miedema's rules suggest that if a transition metal is to form compounds with another metal, they must have a small difference in charge densities at the Wigner-Seitz radius and large difference in work functions [11]. K has a very different work function from Ni and its charge density is too small to form a compound with the latter at ambient conditions. At high pressures, however, due to the *s*-to-*d* transition [13], K behaves like a transition metal with a diffusive *d* orbital that enhances the charge density at the Wigner-Seitz radius and matches that of Ni, allowing the compound to form. Several transition metals are able to form compounds with K at high pressure, a good example being KAg_2 formed at 2–5 GPa [15]. The effects of temperature on compound formation were investigated by subjecting a solid solution of K and Ni to heating at 37 GPa using *ab initio* MD [35]. The simulation reveals a tendency for bond formation with rising temperature. At the synthesis temperature (2500 K), K-Ni-K units are developed throughout the system. This suggests that the formation of bonding in the crystal is facilitated by high temperature mainly through a decrease in the nearest-neighbor distances. Moreover, Bader charge analysis [40] reveals that the $P2_1/m$-K_2Ni is also stabilized through notable electron transfer from K to Ni upon its formation. The Ni atom strips each of the two K atoms of $0.4\,e^-$ thereby inducing strong electrostatic interaction in the crystal. The charge transfer in K_2Ni likely takes place between K 4*s* states and Ni 3*d* states. According to previous theoretical

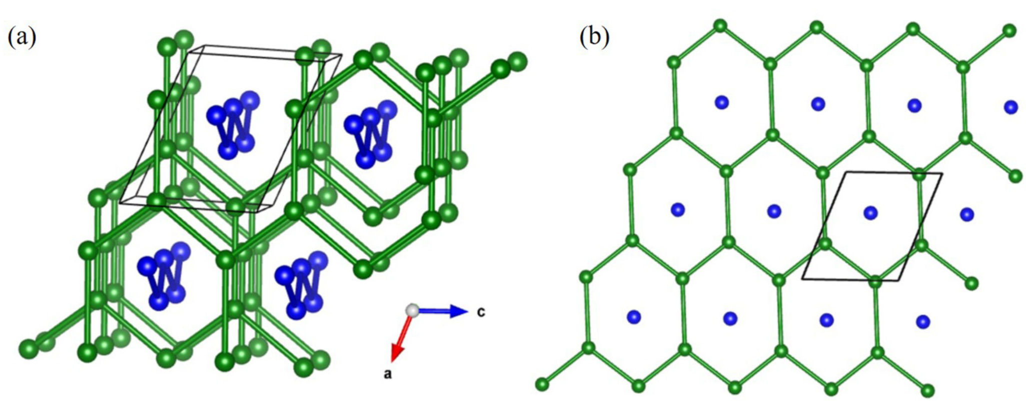

FIG. 2. (a) Crystal structure of $P2_1/m$-K_2Ni. (b) A single layer with K forming distorted honeycomb lattice and Ni occupying vertices. K and Ni atoms are colored green and blue, respectively. Unit cell is drawn black.

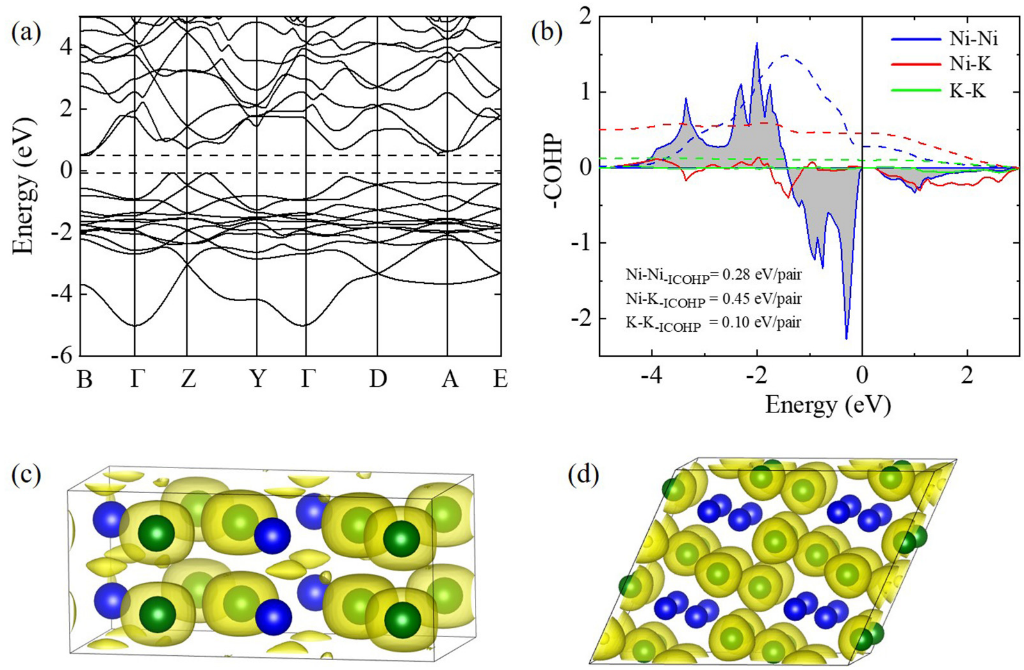

FIG. 3. (a) Electronic band structure and (b) calculated −COHP (solid) and −ICOHP (dashed) curves of Ni-Ni, Ni-K, and K-K pairs of $P2_1/m$-K_2Ni. Electron localization function (isovalue = 0.6) of (c) ideal *Cmcm* structure and (d) $P2_1/m$ structure of K_2Ni. K and Ni atoms are colored green and blue, respectively. All calculations were carried out using HSE functional at 37 GPa, i.e., the synthesis pressure for K-Ni compound [19].

study [41], Ni can become highly electronegative and act like an oxidant at around 50 GPa. Thus, the behavior of Ni under pressure is very different from that under ambient pressure conditions where it is usually cationic in compounds. When it is compressed, the 3*d* orbital in Ni is expected to move completely below the 4*s* orbital which leaves the partially filled 3*d* band below the band gap and forms an electron acceptor [42]. Similar electrostatic stabilization through charge transfer was previously found in K-In [16], Xe-Ni/Fe [43,44], Ar-Ni [45], and K-Fe [46] compounds at high pressure.

A very interesting phenomenon discovered is that $P2_1/m$-K_2Ni exhibits a semiconducting ground state even though both constituents are good metals. The calculated band gap is indirect and the size (∼0.65 eV) is within the infrared spectrum [Fig. 3(a)]. The band-gap opening is induced by a structural distortion of the high symmetric parent structure. In $P2_1/m$-K_2Ni, K atoms form two-dimensional (2D) distorted honeycomb lattices with one translation direction significantly elongated [Fig. 2(b)]. Ni atoms occupy the lattice vertices on the same plane. Electronic DOS calculation shows that an individual 2D lattice of this geometry is metallic. In the crystalline phase, if the stacking of the 2D lattices had no relative translations, i.e., the layers are on top of each other, the resulting three-dimensional (3D) structure would have degenerated bands at the Fermi level and a metallic state as well [Fig. S7(a) in the Supplemental Material [35]]. In this case, the Ni atoms would form a linear chain, highly symmetrical but not corresponding to maximum interaction. Such an ideal structure has a *Cmcm* space group, which can be broken to $P2_1/m$ with stabilization by a symmetry-lowering distortion. As detailed in the Supplemental Material [35], the distortion breaks the degeneracy of the bands at the Fermi level, i.e., some of the degenerate levels are stabilized, the others are destabilized, resulting in a band-gap opening at the Fermi level. Specifically, in $P2_1/m$-K_2Ni, there is a relative displacement between the neighboring 2D lattices along the elongated direction by an amount approximately half of the K-K distance. This causes each 2D lattice to be halfway between the two neighboring lattices and therefore changes the chains of Ni atoms to a zigzag shape, which propagate along the channels within the lattices. This distortion causes the band-gap opening in $P2_1/m$-K_2Ni, as shown in the electronic DOS [Fig. S7(b) in [35]]. This observation confirms the argument that the displacement of the honeycomb K layer and the formation of zigzag Ni chains open a band gap, which is consistent with the Peierls distortion, the solid-state counterpart of the Jahn-Teller effect. For a two-layer system, the displaced stacking corresponds to an energy minimum since it minimizes the repulsion between inner-shell electrons of atoms on neighboring planes [35]. In real space, the degeneracy in ideal *Cmcm* structure results in a small fraction of electrons being pushed out of K atoms, which then occupies interstitial regions between the adjacent 2D lattices, forming an electride state [Fig. 3(c)]. These electrons are accommodated by the quantized orbitals of the interstitial space, which are only energetically accessible at high pressure [47]. However, this effect is very moderate in K_2Ni, as seen from the low ELF value (0.6) for the electride states. In $P2_1/m$-K_2Ni, on the other hand, the interstitial space is significantly reduced due to the shifting and meshing of neighboring layers, which increases the energy for the virtual orbital. As a result, electrons do not populate

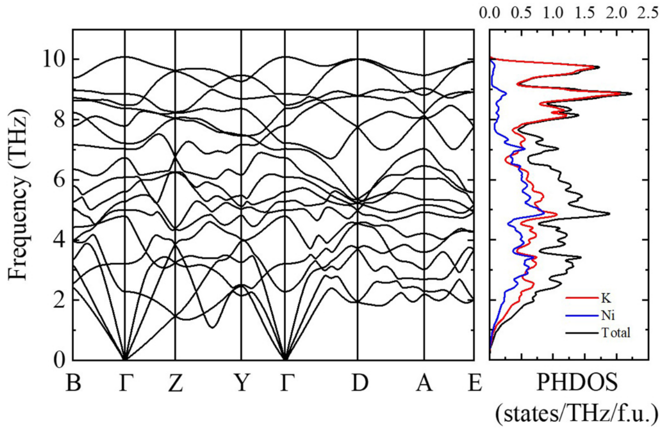

FIG. 4. Phonon dispersion relations and projected phonon density of states for $P2_1/m$-K_2Ni calculated at 37 GPa.

the interstitial sites but instead occupy the Ni-3d orbital which is relatively lower in energy. As shown in Fig. 3(d), the ELF isosurface (0.6) shows no obvious tendency of electron localization, either electrides or covalent bonds, in the structure.

Spin-polarized quantum calculation was performed on a 2×2×2 supercell of $P2_1/m$-K_2Ni as shown in the Supplemental Material [35]. The result reveals that this structure has a ferromagnetic ground state in which all spins on Ni atoms are aligned parallel. The ferromagnetic configuration is ∼0.9 meV/atom lower than the ferrimagnetic configuration (in which spins of unequal magnitudes align in an antiparallel configuration), and ∼1.2 meV/atom lower than the paramagnetic, antiferromagnetic, and nonmagnetic configurations. The calculated −COHP and its integral −ICOHP curves for Ni-Ni, Ni-K, and K-K pairs in $P2_1/m$-K_2Ni are displayed in Fig. 3(b). The Ni-K interaction exhibits the highest −ICOHP value (0.45 eV/pair), which is ionic in nature and contributes to the stabilization of K_2Ni. The K-K interaction on the other hand is very weak, as seen from the low −ICOHP value (0.10 eV/pair). In the −COHP curve, Ni-Ni pairs show the bonding states in the energy region from −4.8 to −1.4 eV, and antibonding states from −1.4 eV to the Fermi level. These states are attributed to the interaction between highly occupied 3d orbitals, which is commonly seen in late transition metals. A similar antibonding feature was also observed in other transition metals containing compounds with highly occupied d orbitals, e.g., $LiAg_2Sn$ [48] and LaAuSb [49]. A manifestation of this electron instability is the band-gap opening at the Fermi level, a natural way to deplete the antibonding area through structural distortion. Another response to the instability is electronic structure distortion, which rearranges electrons into two inequivalent spin sublattices, thereby lowering the total energy and giving rise to ferromagnetism [35]. The dynamical stability of $P2_1/m$-K_2Ni was established through the calculation of phonon-dispersion relations, which show no imaginary frequencies throughout the BZ. The phonon DOS projected on K and Ni reveals that the vibrations of the two atoms are coupled strongly in the low-frequency region (see Fig. 4). In the high-frequency region, vibrational modes are predominantly due to K atoms. The vibrational DOS calculated at finite temperatures shows that the $P2_1/m$-K_2Ni is stable at room temperature as well, but it has a tendency to melt when the temperature is raised above 2000 K [35]. For a monoclinic system, $P2_1/m$-K_2Ni fulfills the Born-Huang criterion [37] for mechanical stability. Using the Voigt-Reuss-Hill approximation [50], the $P2_1/m$-K_2Ni is calculated to have a bulk modulus of 98.6 GPa ± 1.17 GPa, shear modulus of 20.1 GPa ± 10.77 GPa, and a bulk/shear ratio of 4.9 ± 0.11, indicating that this material is ductile in nature.

IV. CONCLUSIONS

In conclusion, we predict a stable compound of K_2Ni formed at 37 GPa. The predicted monoclinic structure is identified as the long-sought structure of the K-Ni compound that was synthesized two decades ago, and the only K-Ni compound known to date. The simulated x-ray-diffraction pattern of the proposed K_2Ni structure matches well with the experiment, and the phonon calculation establishes its dynamics stability. K_2Ni is calculated to have a ferromagnetic and semiconducting ground state, albeit both constituents are good metals. Electron instability due to the degeneracy at the Fermi level causes significant Peierls distortion in the structure, which reduces the crystal symmetry and opens a small band gap of 0.65 eV. The fact that K can be incorporated with Ni at high-pressure conditions is important for understanding the partition of trace elements between the core and mantle, a key problem in the evolution of Earth.

ACKNOWLEDGMENTS

This project was supported by Natural Sciences and Engineering Research Council of Canada (NSERC). Computing resource is provided by University of Saskatchewan, Westgrid, and Compute Canada. Part of this work was performed under the auspices of the U.S. Department of Energy by Lawrence Livermore National Security, LLC under Contract No. DE-AC52-07NA27344.

[1] E. Wigner and F. Seitz, Phys. Rev. **43**, 804 (1933).
[2] E. Wigner and H. B. Huntington, J. Chem. Phys. **3**, 764 (1935).
[3] N. W. Ashcroft, Phys. Rev. Lett. **21**, 1748 (1968).
[4] R. P. Dias and I. F. Silvera, Science **355**, 715 (2017).
[5] M. I. Eremets, A. P. Drozdov, P. P. Kong, and H. Wang, Nat. Phys. **15**, 1246 (2019).
[6] P. Loubeyre, F. Occelli, and P. Dumas, Nature (London) **577**, 631 (2020).
[7] J. B. Neaton and N. W. Ashcroft, Nature (London) **400**, 141 (1999).
[8] T. Matsuoka and K. Shimizu, Nature (London) **458**, 186 (2009).
[9] Y. Ma, M. Eremets, A. R. Oganov, Y. Xie, I. Trojan, S. Medvedev, A. O. Lyakhov, M. Valle, and V. Prakapenka, Nature (London) **458**, 182 (2009).
[10] M. Hanfland, K. Syassen, N. E. Christensen, and D. L. Novikov, Nature (London) **408**, 174 (2000).

[11] A. R. Miedema, P. F. de Chatel, and F. R. de Boer, Physica B (Amsterdam, Neth.) **100**, 1 (1980).
[12] M. Miao, Y. Sun, E. Zurek, and H. Lin, Nat. Rev. Chem. **4**, 508 (2020).
[13] M. S. T. Bukowinsky, Geophys. Res. Lett. **3**, 491 (1976).
[14] C. J. Pickard and R. J. Needs, Phys. Rev. Lett. **107**, 087201 (2011).
[15] T. Atou, M. Hasegawa, L. J. Parker, and J. V. Badding, J. Am. Chem. Soc. **118**, 12104 (1996).
[16] Y. Liu, C. Wang, P. Lv, H. Sun, D. Duan, and X. Wang, Solid State Commun. **287**, 77 (2019).
[17] K. A. Geottel, Geophys. Surv. **2**, 369 (1976).
[18] G. J. Wasserburg, G. J. F. MacDonald, F. Hoyle, and W. A. Fowler, Science **143**, 465 (1964).
[19] L. Parker, T. Atou, and J. Badding, Science **273**, 95 (1996).
[20] K. K. M. Lee and R. Jeanloz, Geophys. Res. Lett. **30**, 2212 (2003).
[21] K. K. M. Lee, G. Steinle-Neumann, and R. Jeanloz, Geophys. Res. Lett. **31**, L11603 (2004).
[22] Y. Yao, J. S. Tse, and K. Tanaka, Phys. Rev. B **77**, 052103 (2008).
[23] Y. Wang, J. Lv, L. Zhu, and Y. Ma, Phys. Rev. B **82**, 094116 (2010).
[24] Y. Wang and Y. Ma, Comput. Phys. Commun. **183**, 2063 (2012).
[25] G. Kresse and J. Hafner, Phys. Rev. B **47**, 558 (1993).
[26] G. Kresse and D. Joubert, Phys. Rev. B **59**, 1758 (1999).
[27] J. P. Perdew, K. Burke, and M. Ernzerhof, Phys. Rev. Lett. **77**, 3865 (1996).
[28] A. Togo, F. Oba, and I. Tanaka, Phys. Rev. B **78**, 134106 (2008).
[29] Y. Yao, R. Martoňák, S. Patchkovskii, and D. D. Klug, Phys. Rev. B **82**, 094107 (2010).
[30] J. Heyd, G. E. Scuseria, and M. Ernzerhof, J. Chem. Phys. **118**, 8207 (2003).
[31] S. Maintz, V. L. Deringer, A. L. Tchougréeff, and R. Dronskowski, J. Comput. Chem. **37**, 1030 (2016).
[32] S. L. Dudarev, G. A. Botton, S. Y. Savrasov, C. J. Humphreys, and A. P. Sutton, Phys. Rev. B **57**, 1505 (1998).
[33] G. W. Mann, K. Lee, M. Cococcioni, B. Smit, and J. B. Neaton, J. Chem. Phys. **144**, 174104 (2016).
[34] K. Momma and F. Izumi, J. Appl. Cryst. **44**, 1272 (2011).
[35] See Supplemental Material at http://link.aps.org/supplemental/10.1103/PhysRevB.102.134120 for the analysis of energy, electronic structure, phonon, thermal stability, and mechanic stability for candidate structures of K_2Ni, which includes Refs. [36–38].
[36] Y. Yao and D. D. Klug, Phys. Rev. B **81**, 140104(R) (2010).
[37] M. Born and K. Huang, *Dynamical Theory of Crystal Lattices* (Clarendon Press, Oxford, 1956).
[38] F. Mouhat and F. X. Coudert, Phys. Rev. B **90**, 224104 (2014).
[39] P. Pavone, S. Baroni, and S. de Gironcoli, Phys. Rev. B **57**, 10421 (1998).
[40] R. F. W. Bader, *Atoms in Molecules—A Quantum Theory* (Oxford University Press, Oxford, 1990).
[41] X. Dong, A. R. Oganov, G. Qian, X-F. Zhou, Q. Zhu, and H.-T. Wang, arXiv:1503.00230.
[42] A. K. McMahan and R. C. Albers, Phys. Rev. Lett. **49**, 1198 (1982).
[43] E. Stavrou, Y. Yao, A. F. Goncharov, S. S. Lobanov, J. M. Zaug, H. Liu, E. Greenberg, and V. B. Prakapenka, Phys. Rev. Lett. **120**, 096001 (2018).
[44] K. K. M. Lee and G. Steinle-Neumann, J. Geophys. Res. **111**, B02202 (2006).
[45] A. A. Adeleke, M. Kunz, E. Greenberg, V. B. Prakapenka, Y. Yao, and E. Stavrou, ACS Earth Space Chem. **3**, 2517 (2019).
[46] A. A. Adeleke and Y. Yao, J. Phys. Chem. A **124**, 4752 (2020).
[47] M. S. Miao and R. Hoffmann, Acc. Chem. Res. **47**, 1311 (2014).
[48] Z. Wu, R. D. Hoffmann, D. Johrendt, B. D. Mosel, and H. Eckert, J. Mater. Chem. **13**, 2561 (2003).
[49] E. M. Seibel, L. M. Schoop, W. Xie, Q. D. Gibson, J. B. Webb, M. K. Fuccillo, J. W. Krizan, and R. J. Cava, J. Am. Chem. Soc. **137**, 1282 (2015).
[50] R. Hill, Proc. Phys. Soc. (London) **65**, 349 (1952).